Available online at www.sciencedirect.com
ScienceDirect
European Journal of Medicinal Chemistry 42 (2007) 1263–1271
EUROPEAN JOURNAL OF MEDICINAL CHEMISTRY
http://www.elsevier.com/locate/ejmech

Original article

Synthesis, biological evaluation and molecular modeling studies of arylidene-thiazolidinediones with potential hypoglycemic and hypolipidemic activities

Lúcia Fernanda C. da Costa Leite [a], Rosa Helena Veras Mourão [b], Maria do Carmo Alves de Lima [b], Suely Lins Galdino [b], Marcelo Zaldini Hernandes [c], Francisco de Assis Rocha Neves [d], Stéphanie Vidal [e], Jacques Barbe [e], Ivan da Rocha Pitta [b,*]

[a] *Departamento de Química, Universidade Católica de Pernambuco, Brazil*
[b] *Departamento de Antibióticos, Universidade Federal de Pernambuco, CEP 50670-901 Recife, Pernambuco, Brazil*
[c] *Ciências Farmacêuticas, Universidade Federal de Pernambuco, CEP 50670-901 Recife, Pernambuco, Brazil*
[d] *Universidade de Brasília, CEP 70910-900 Brasília, DF, Brazil*
[e] *GERCTOP, UMR CNRS 6178, Université de la Méditerranée, Faculté de Pharmacie, 13385 Marseille Cedex 5, France*

Received 16 June 2006; received in revised form 21 December 2006; accepted 12 February 2007
Available online 3 March 2007

Abstract

New arylidene-thiazolidinediones (ATZDs) were synthesized and evaluated in the alloxan-induced hyperglycemia mice model. The molecular target taken into consideration is the nuclear PPAR-γ whose crystallographic structure is available on the PDB database as 2PRG. Thus the hypoglycemic and hypolipidemic activities of compounds were compared with the result of their docking after removal of the co-crystallized ligand present in the 2PRG structure. Molecular modeling studies were carried out using the Autodock 3.0.5 and ADT 1.1 programs.

Keywords: Arylidene-thiazolidinediones; Hypoglycemic; Hypolipidemic; Molecular modeling; Docking

1. Introduction

Diabetes mellitus is a chronic multifactorial metabolic disease characterized by insulin resistance, hyperglycemia, and often hyperlipidemia. TZDs are known to be insulin sensitizers and have been developed and clinically used as antidiabetic agents. The maleate of rosiglitazone, a medicine of the TZDs' class, showed significant clinical efficacy against DM type 2. The disease is associated with obesity, dislipidemia and hypertension, leading to increased cardiovascular risks[1]. Untreated, type 2 diabetes leads to several chronic diseases such as retinopathy, nephropathy, and cardiovascular diseases, the latter leading to increased mortality [2]. Owing to the forecasted epidemic in DM type 2, the increasing financial and social costs, and the complicated pathology of the disease, new therapies are needed that address both insulin resistance and the dislipidemic components of the disease [3–5]. It was discovered empirically decades ago that two classes of compounds known as thiazolidinediones and fibrates, possess the ability to lower the blood glucose and lipids levels in rodent models of insulin resistance and hyperlipidemia, respectively. In humans, the

Abbreviations: ADT, auto docking tools; ATZDs, arylidene-thiazolidinediones; DM, diabetes mellitus; LBD, ligand binding domain; PG, plasmatic glucose level; PPAR, peroxisome proliferator-activated receptor; TDZs, thiazolidinediones; TG, plasmatic triglyceride level.

* Corresponding author. Tel.: +55 81 21268347; fax: +55 81 21268346.
E-mail address: irpitta@gmail.com (I. da Rocha Pitta).

0223-5234/$ - see front matter © 2007 Elsevier Masson SAS. All rights reserved.
doi:10.1016/j.ejmech.2007.02.015

fibrates are effective in lowering serum triglycerides and raising HDL cholesterol levels, primarily through increased clearance and decreased synthesis of triglyceride-rich VLDL. Fibrates have been shown to slow the progression of atherosclerosis and reduce the number of coronary events in secondary prevention studies and in patients with normal levels of LDL cholesterol and, recently, in diabetic patients [2]. TZDs have been shown to reduce plasmatic glucose, lipid, and insulin levels, and can be used for treatment of the DM type 2 [6,7]. The target of TZDs has been identified as the peroxisome proliferator-activated receptor γ and the glucose-lowering action of the TZDs has been shown to be closely related to their PPAR-γ agonist activity. TZDs enhance adipocyte differentiation and increase the insulin sensitivity of tissues [8]. Insulin sensitizers PPAR-γ agonists, such as pioglitazone and rosiglitazone (Fig. 1) have a range of clinical effects including improvement of insulin sensitivity and glucose tolerance and lowering of blood glucose levels in type 2 diabetic patients [9,10].

Several structures of the PPAR-γ/ligand binding domain have been portrayed using X-ray crystallography and have been reported in the literature. Some examples include the structures of the apo-PPAR-γ LBD, a ternary complex of LBD with a TZD (rosiglitazone) and an 88 amino acid fragment of the coactivator SRC1 [11,12] and LBD complexes with a partial agonist GW0072 (thiazolidine acetamide derivative) [13]. The identification of the nuclear PPAR-γ and PPAR-α as the primary targets for the normoglycemic TZDs and the lipid lowering fibrates, respectively, has provided new opportunities for the identification of novel compounds for the treatment of type 2 diabetes [14]. The present work describes the synthesis and gives the structural characteristics of 12 ATZDs derived from the 5-benzylidene-3-(4-methyl-benzyl)-thiazolidine-2,4-dione substituted on the benzylidene moiety [15]. These compounds were evaluated after oral administration at different doses in hyperglycemic mice with alloxan-induced diabetes. The plasmatic glucose and the triglyceride levels were measured and compared with those when rosiglitazone is used as reference drug. Despite the fact that the pharmacological mechanism was not determined for these ATZDs, our results, based upon the similarity between these molecules and previously investigated ATZDs, strongly support the hypothesis that these compounds could act through the PPAR-γ. So, we will consider this hypothesis during this work. The structure of the complexes formed between these compounds and PPAR-γ and PPAR-α LBD was modelled and their interactions analysed, using Autodock 3.0.5 and ADT 1.1 (Auto docking tools) programs.

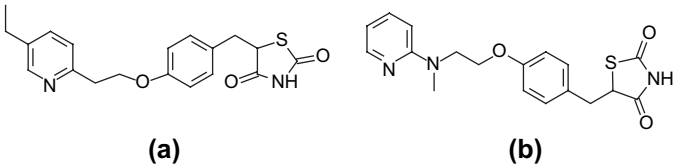

Fig. 1. Pioglitazone (a) and rosiglitazone (b).

2. Chemistry

The 5-arylidene-3-(4-methyl-benzyl)-thiazolidine-2,4-diones, **1**–**12**, were prepared by nucleophilic addition of the 3-(4-methyl-benzyl)-thiazolidine-2,4-dione on selected aryl-substituted ethyl-(2-cyano-3-phenyl)-acrylates. The synthetic pathways are illustrated in Scheme 1. Thiazolidine-2,4-dione, was N-(3)-alkylated in the presence of potassium hydroxide, which enables the thiazolidine potassium salt to react with benzyl halide in a hot alcohol medium.

Arylidene-thiazolidinediones were isolated in a single isomer form. X-ray crystallographic studies and ^{13}C NMR have demonstrated the preferred *Z* configuration for 5-arylidene-thiazolidinones [16–18]. Melting points were measured in a capillary tube on Buchi (or Quimis) apparatus. Thin layer chromatography was performed on silica gel plates Merck 60F254. Infrared spectra of 1% KBr pellets were recorded on a Perkin Elmer 1310 spectrometer for compounds **2**, **6**, **7** or Bruker IFS66 spectrometer for **8**, **12**. ^{1}H NMR spectra were recorded on a Bruker AC 300 P spectrophotometer in DMSO-d_6 as solvent, with tetramethylsilane as internal standard. Mass spectra were recorded on a Delsi–Nermag R 1010 C spectrometer. The already published chemical data of **1**, **3**–**5**, **9**–**11** [19], are not reported here.

3. Biological activity

The effects of the new ATZDs prepared were evaluated using the experimental model of diabetes induced by alloxan. The biological activity in vivo was evaluated with daily doses of 5–40 mg/kg administered orally for 15 days of treatment, and specific reduction in levels of PG and TG was measured for the diabetic groups treated with the ATZDs compared to the diabetic group treated with vehicle (CMC 0.25%). Rosiglitazone was used as reference drug at doses of 5–30 mg/kg/day. Hyperglycemia was induced by alloxan monohydrate at 80 mg/kg p.o. dose. After 10 days of treatment, mice with 200–350 mg/dL PG level and 100–250 mg/dL TG level were selected for further experiments. Blood samples were regularly collected from the animals after they had been fed between 8 h and 10 h in the morning, the blood being taken from the retro-orbital plexus under a light anaesthetic (ethyl ether), 1 h after the administration of the compounds at different days throughout the treatment (1, 3, 10 and 15 days). Levels of plasmatic glucose and triglycerides were analysed using commercially available kits (LABTEST – Brazil), based on enzymatic methods.

The hypoglycemic and hypolipidemic effects after oral administration of ATZDs in mice with alloxan-induced diabetes are summarized in Table 1 and portrayed in Graphs 1 and 2, which show the results in terms of percentage reduction of GP and TG levels, obtained from samples of blood collected before and after 15 days of treatment in animals treated with ATZDs, rosiglitazone and vehicle. The values are the average ones ± standard error ($N = 6$) for each experimental group. With the exception of 5-(3-chloro-benzylidene)-3-(4-methyl-benzyl)-thiazolidine-2,4-dione **6**, the dose of 10 mg/kg/day

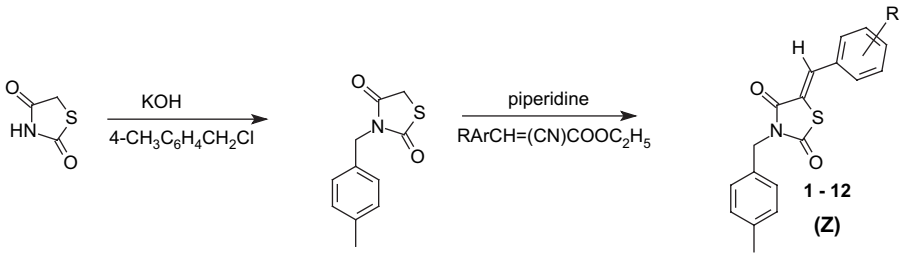

Scheme 1. Synthetic pathways of arylidene-thiazolidinediones.

reduced significantly the GP levels ($p < 0.05$) after 15 days of treatment.

4. Theoretical calculations

The structures and conformational analysis of arylidene-thiazolidinediones **1–12** were obtained by the application of AM1 method [20] available in the BioMedCAChe software [BioMedCAChe version 6.1, Copyright ©2000–2003 Fujitsu Limited, Copyright©1989–2000, Oxford Molecular Ltd., http://www.CACheSoftware.com], using internal default settings for convergence criteria. The results obtained in these calculations confirm the greater stability of the *Z* isomer in all cases.

The docking analysis was firstly carried out on the PPAR-γ binding site in the 2PRG [11] obtained from the RCSB Protein Data Bank, http://www.rcsb.org/pdb, where the residues were bonded more closely to the rosiglitazone agonist, co-crystallized with PPAR-γ. In this crystal structure, the LBD forms a homodimer in which both monomers have nearly identical Cα conformations. The structure of the "A" monomer of the LBD homodimer was chosen as the target for docking studies.

Table 1
Dose–response effect of the ATZDs **1–12** (see Scheme 1) in mice with alloxan-induced diabetes

#	R	Dose (mg/kg/day)	% Reduction,[a] PG (mg/dL)	% Reduction,[a] TG (mg/dL)
1	4-Cl	10	18.7, $p < 0.002$	NS
		30	22.8, $p < 0.002$	48, $p < 0.001$
		40	31.5, $p < 0.02$	27.1, $p < 0.01$
2	4-OH	10	19.9, $p < 0.008$	NS
		30	37.3, $p < 0.04$	NS
		40	37.2, $p < 0.001$	NS
3	2-Cl	10	19.2, $p < 0.05$	14.8, $p < 0.05$
		20	47, $p < 0.001$	20, $p < 0.01$
		30	43.3, $p < 0.05$	26, $p < 0.01$
4	4-OCH_3	5	27.2, $p < 0.001$	32.2, $p < 0.01$
		10	20.6, $p < 0.07$	37.6, $p < 0.01$
		30	50.8, $p < 0.00003$	58.8, $p < 0.04$
5	2.4-OCH_3	10	21.8, $p < 0.01$	40, $p < 0.01$
		30	34.6, $p < 0.001$	46.5, $p < 0.01$
		40	20.1, $p < 0.025$	NS
6	3-Cl	10	NS	NS
7	4-CH_3	10	16.3, $p < 0.025$	41.7, $p < 0.020$
8	3-Br	10	21.3, $p < 0.001$	17.6, $p < 0.05$
9	4-$N(CH_3)_2$	10	14.9, $p < 0.01$	NS
		20	35.8, $p < 0.025$	17.4, $p < 0.01$
		30	40.8, $p < 0.001$	44.1, $p < 0.001$
10	4-$C_6H_5CH_2O$	10	9.37, $p < 0.05$	43.6, $p < 0.05$
		20	27.7, $p < 0.001$	45.2, $p < 0.025$
		30	20.2, $p < 0.0001$	42.1, $p < 0.01$
11	4-F	30	13.5, $p < 0.05$	NS
12	4-NO_2	30	11.42, $p < 0.05$	7.1, $p < 0.05$
Rosiglitazone		5	26.3, $p < 0.001$	15.9, $p < 0.05$
		10	36.7, $p < 0.001$	43.3, $p < 0.001$
		30	11.6, $p < 0.05$	6.4, $p < 0.05$
Diabetic + CMC, average of 11 groups with $n = 6$		0.1 mL/10 g	T0 462.4 ± 25, T15 474.9 ± 22.3, NS	T0 209.6 ± 31.3, T15 199.8 ± 21.5, NS
Normoglycemic + CMC, average of 11 groups with $n = 6$		0.1 mL/10 g	T0 126.5 ± 7.6, T15 124.2 ± 6.8, NS	T0 118.2 ± 10.2, T15 111.4 ± 9, NS
Normoglycemic with $n = 6$		–	T0 129.5 ± 5, T15 131 ± 7, NS	T0 128.7 ± 7.3, T15 125 ± 14, NS

[a] The reduction percentage was calculated using the equation: $1 - [(TT/0T)/(TC/0C)] \times 100$; TT: treated test at the d-day; 0T: treated test at the day zero; TC: control at the d-day; 0C: control at the day zero; NS: not significant; T0: time zero; T15: after 15 days of treatment. Each value is an average one ± standard error with $n = 6$ animals. Differences between day zero and day 15 were considered significant if $p \leq 0.05$.

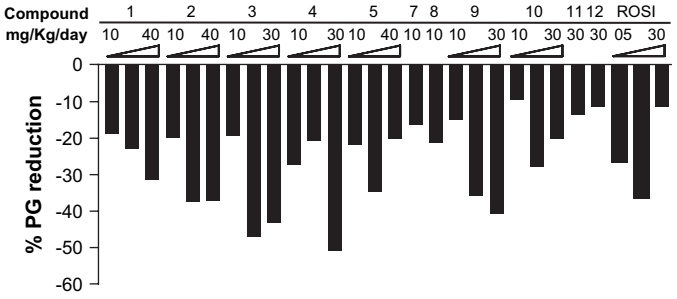

Graph 1. Percentage of PG reduction with ATZDs and rosiglitazone (see details in Table 1 and results of **6** are not shown because of no significance).

The rosiglitazone agonist was extracted from the complex, and, during the calculations, the active site was determined within a cubic box centered on the co-crystallized ligand (coordinates: $X = 50.140$; $Y = -38.202$; $Z = 19.559$) with edges of 22.5 Å, thereby ensuring that the active site region was covered. Within this pre-defined region, the grids of probe atom interaction energies were computed with a default resolution of 0.375 Å and the ligands were then docked by genetic algorithm followed by a local search procedure (GA-LS), also known as a Lamarckian genetic algorithm (LGA) [21], and the 50 lowest energy structures were stored for further analysis.

The docking analyses of compounds **1**–**12** and rosiglitazone were carried out by means of the Autodock tools [22] (ADT) v1.1 and Autodock v3.0.5 program [Autodock, Autogrid, Autotors, Copyright©1991–2000, The Scripps Research Institute, http://www.scripps.edu/mb/olson/doc/autodock], and using the internal default parameters for all the variables, except for the number of docking runs (50), the maximum number of energy evaluations on genetic algorithm – GA (25,000,000) and the maximum number of generations in GA (5000). Preliminary calculations indicate that modifications of these three specific parameters give a significant improvement in the results, contributing to more stable conformations of the ligands. The active site was considered as a rigid molecule, whereas the ligands were treated as being flexible, i.e. all non-ring torsions were allowed. This approach seems to be coherent with the structural similarity observed between rosiglitazone and compounds under investigation.

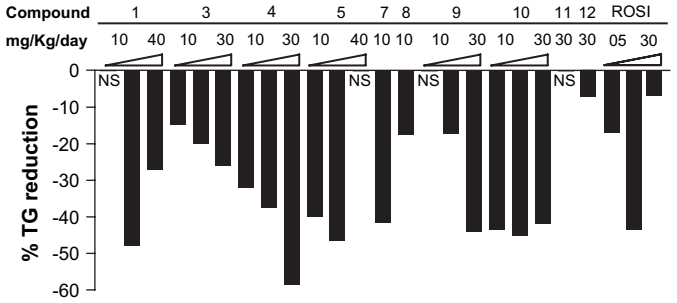

Graph 2. Percentage of TG reduction with ATZDs and rosiglitazone (see details in Table 1 and results of **2** and **6** are not shown because of no significance).

The docking procedure for the PPAR-α binding site basically follows the same setup shown for PPAR-γ. The "A" chain of the structure 1K7L [23] from the RCSB Protein Data Bank, was used as the target. The GW409544 (Propionic acid derivative) agonist co-crystallized with PPAR-α in structure 1K7L was used to define the active site, centered at coordinates ($X = -17.866$; $Y = -13.599$; $Z = -3.726$).

5. Results and discussion

The most stable docking solutions for the ATZDs **1**–**12** complexed with the PPAR-γ LBD and PPAR-α LBD are listed in Table 2, along with the free energy of binding (ΔG) values.

According to the crystal structure of rosiglitazone in the LBD of PPAR-γ, the thiazolidine ring establishes several specific interactions with neighboring amino acids of the LBD. These interactions include hydrogen bonding with amino acids H323, H449 and Y473, as reported in the literature [1,8].

The docking studies started with rosiglitazone, for which the binding mode has been determined experimentally [8]. Autodock was successful in reproducing the binding position for rosiglitazone, showing a RMS deviation of 0.8 Å in comparison with the experimental geometry when this TDZ is co-crystallized in the PPAR-γ and the same patterns for hydrogen bonding.

The binding profile of the 5-arylidene-3-benzyl-thiazolidine-2,4-dione was compared with the profile of the rosiglitazone molecule. The ligand 5-(4-hydroxy-benzylidene)-3-(4-methyl-benzyl)-thiazolidine-2,4-dione **2**, interacts mainly with PPAR-γ through the formation of two hydrogen bonds between the *para*-hydroxyl group of the benzylidene ring and the histidine H449(A) and the glutamine Q286(A) residues, respectively (Fig. 2). Actually, the histidine H449 residue also interacts with rosiglitazone in the crystal structure through hydrogen bonding [8].

In Fig. 3 the ligand (*Z*) 5-(4-methoxy-benzylidene)-3-(4-methyl-benzyl)-thiazolidine-2,4-dione **4** shows hydrogen bond between the oxygen atom in position 4 of the thiazolidine ring

Table 2
Docking of ATZDs ligands in the PPAR-γ and PPAR-α

ATZD #	R	Free energy of binding (kcal/mol)	
		PPAR-γ	PPAR-α
1	4-Cl	−8.36	−8.56
2	4-OH	−8.90	−8.13
3	2-Cl	−8.61	−7.95
4	4-OCH_3	−8.36	−7.63
5	2.4-OCH_3	−8.22	−7.70
6	3-Cl	−8.61	−8.49
7	4-CH_3	−8.39	−8.44
8	3-Br	−8.86	−8.56
9	4-$N(CH_3)_2$	−8.85	−8.69
10	4-$C_6H_5CH_2O$	−9.58	−9.26
11	4-F	−8.22	−8.26
12	4-NO_2	−10.45	−8.62
Rosiglitazone		−10.22	−13.49

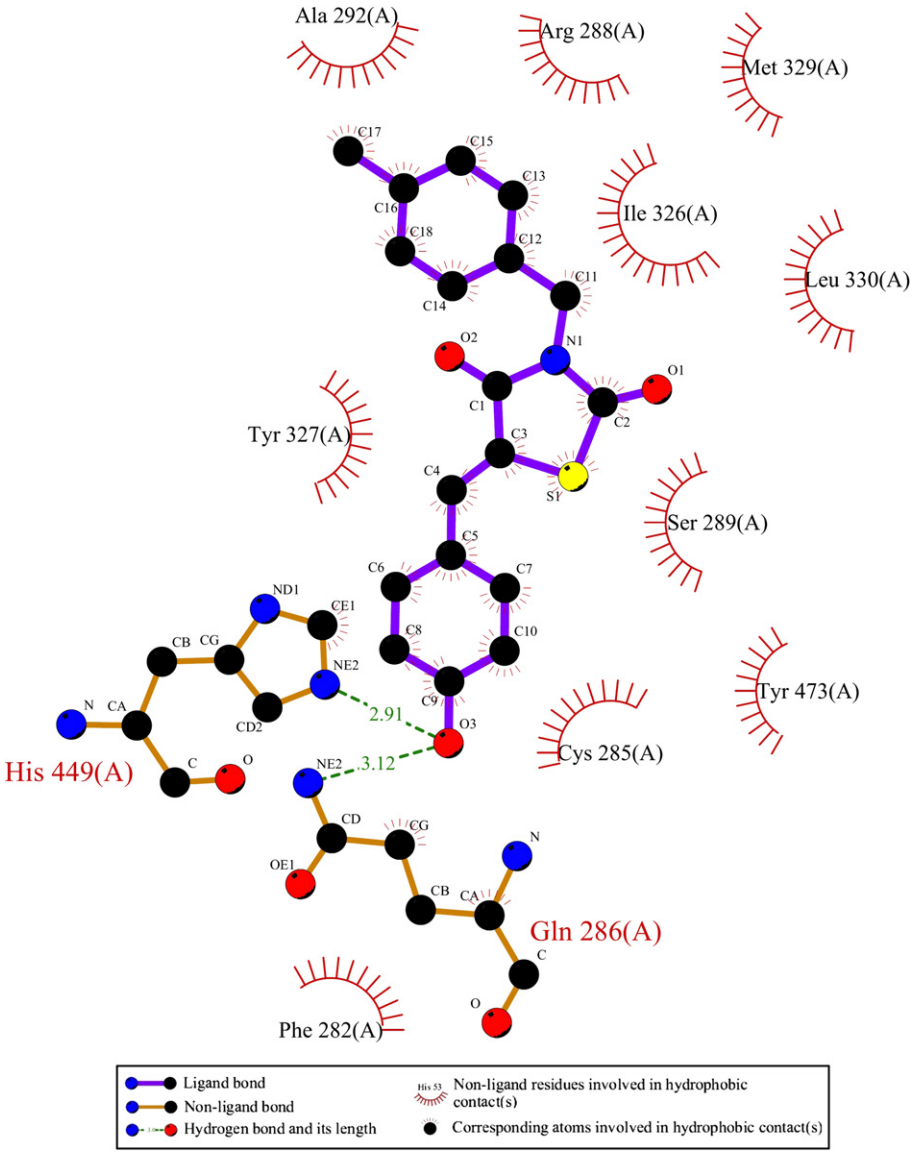

Fig. 2. Main hydrogen bonds between (*Z*) 5-(4-hydroxy-benzylidene)-3-(4-methyl-benzyl)-thiazolidine-2,4-dione **2** and PPAR-γ.

and the histidine His440(A) residue of the PPAR-α. The LIG PLOT program [24] was used to display Figs. 2 and 3.

Fig. 4 shows the ligand (*Z*) 5-(4-hydroxy-benzylidene)-3-(4-methyl-benzyl)-thiazolidine-2,4-dione **2** (green stick model) interacting with the His449(A) and the Gln286(A) PPAR-γ residues (wireframe model) through hydrogen bonding, at measured distances of 1.897 Å and 2.162 Å, respectively. The crystallographic structure of the rosiglitazone ligand (blue stick model) shows interactions with the Ser289(A) and His323(A) residues through hydrogen bonding at distances of 1.932 Å and 1.859 Å, respectively.

In order to verify the robustness of the results, one can see in Fig. 5a the distribution of the docking solutions for ligand **2** in PPAR-γ. The results are organized into 15 clusters (RMS within 0.5), each one with the lowest and mean docking energy and the number of poses. The higher clusters are those ones with the most negative docking energies, showing that the statistics on the docking distributions are favourable for the most stable solutions (most negative docking energies). Fig. 5b shows the superposition of the 50 docking poses (wireframe models), besides the crystallographic structure of the rosiglitazone (stick model). This pattern was observed for the other ligands and targets too. The Figs. 4, 5b and 6 were made with PyMOL v0.99 [25].

A trend was observed between the ATZD (**1**–**4**, **9**) free energy of binding (PPAR-γ) and the values of ED_{40} for PG after 15 days of treatment (Table 3), if we keep the hypothesis of these ATZDs being PPAR-γ ligands. This correlation corroborates the expectation that more stable is the ligand receptor complex or smaller (more negative) the free energy of binding, smaller the value of ED_{40} or greater the potency of the respective molecule. The exception is compound **3** (the 2-Cl derivative), which is the most potent molecule ($ED_{40} = 3.3 \times 10^{-5}$ mol/L), but doesn't show the most stable ligand–receptor complex (−8.61 kcal/mol) with PPAR-γ. Therefore, this correlation is poor, because of the complex character of this comparison. It is important to

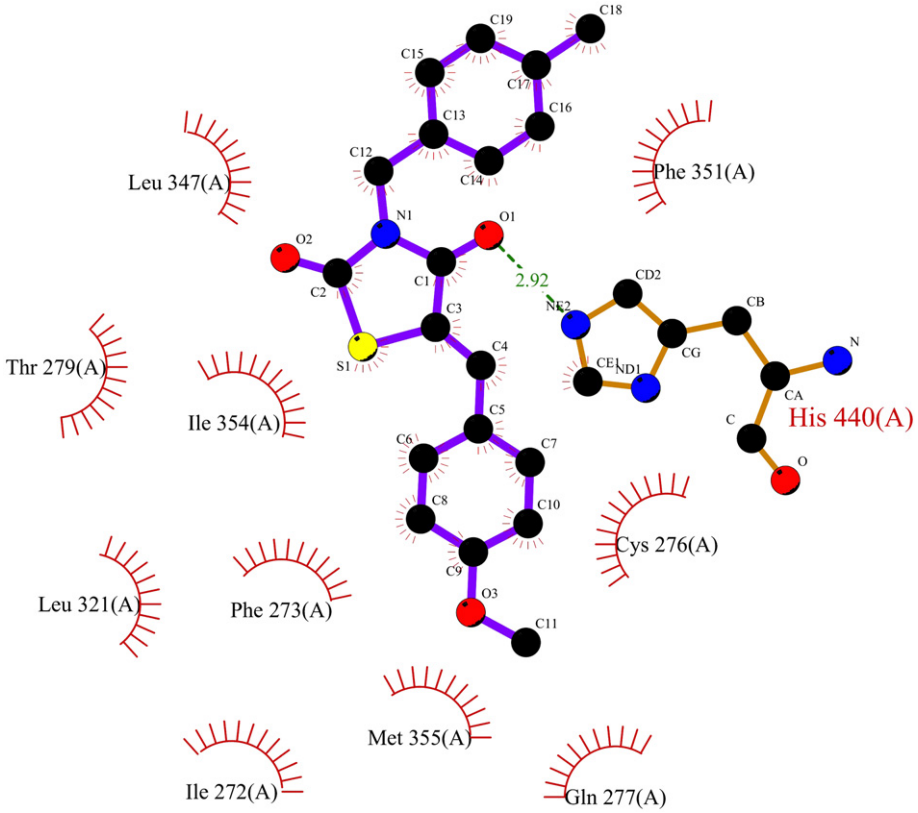

Fig. 3. Hydrogen bond between (*Z*) 5-(4-methoxy-benzylidene)-3-(4-methyl-benzyl)-thiazolidine-2,4-dione **4** and the His440(A) residue of the PPAR-α.

stress that the docking results are related exclusively to the ligand–receptor interaction, while the experimental results (ED_{40}) take into account also the pharmacokinetics (bio-distribution, metabolization, ADMET, etc.). Besides, the docking results obtained here take into account the entropic and solvation effects on the active site only in an indirect way, because of the parametrization of program's internal score function. Additionally, further studies are being carried out in our group, in order to investigate the metabolization pattern of this class of molecules. In such a way, we believe that Autodock is able to reach reliable docking results [26] for the molecular systems presented here.

The effective dose (mg/kg/day) for a 40% reduction (ED_{40}) in the levels of GP and TG for compounds **1**–**4** and **9** was calculated from the dose–response curve for the three doses. The compound **3** (2-Cl) shows the highest capability to reduce the glucose levels. This derivative is 2.09 times more potent than **1**, and 1.69, 1.27 and 1.30 times more potent than compounds **4** (4-OCH_3), **2** (4-OH) and **9** (4-$N(CH_3)_2$), respectively. However, **4** showed the best efficacy since it reduced the blood glucose levels to 51% from baseline, a higher value than that observed with the rosiglitazone treatment (37%). We did not analyze whether the hypoglycemic effects of our compounds were derived from a PPAR agonist effect, since we did not evaluate their direct effects or binding affinities to the PPAR-γ. However, since these ligands show a chemical structure close to that of rosiglitazone, our results strongly suggest that these compounds should have some effects through the PPAR. Preliminary transcription assay, performed on U937 cells where we co-transfected with PPAR-γ expression vector together with a PPAR-γ response element driving a luciferase reporter gene showed that these compounds have an agonist PPAR-γ effect (not shown). Further experiments are going on to address the PPAR-γ and PPAR-α binding affinity together with a dose–response curve in transcription reporter gene assay and the PPAR-γ co-crystallized structure with these ligands.

6. Conclusion

As a general rule, it was observed that, branched substituents on the arylidene ring contribute significantly to the biological activity, while the ATZDs with electron donor groups in the position 4 produce a significant reduction in the glucose levels.

After the analyses of docking and biological data, it became possible to conclude that the presence of the chlorine in position 4 or 2 at the phenyl ring, as observed in the (*Z*) 5-(4-chloro-benzylidene)-3-(4-methyl-benzyl)-thiazolidine-2,4-dione **1** and the (*Z*) 5-(2-chloro-benzylidene)-3-(4-methyl-benzyl)-thiazolidine-2,4-dione **3**, could play an important role in explaining the hypoglycemic and hypolipidemic activities. The chlorine atom in position 3 plays the opposite role, as observed with the (*Z*) 5-(3-chloro-benzylidene)-3-(4-methyl-benzyl)-thiazolidine-2,4-dione **6**. At a dose of 10 mg/kg/day, chlorine in position 2 (or 4) reduces the levels of GP by 19%, while the same in position 3, does not show significant results. One can see the docking poses for ligands **1**, **3** and **6** in Fig. 6. A detailed analysis

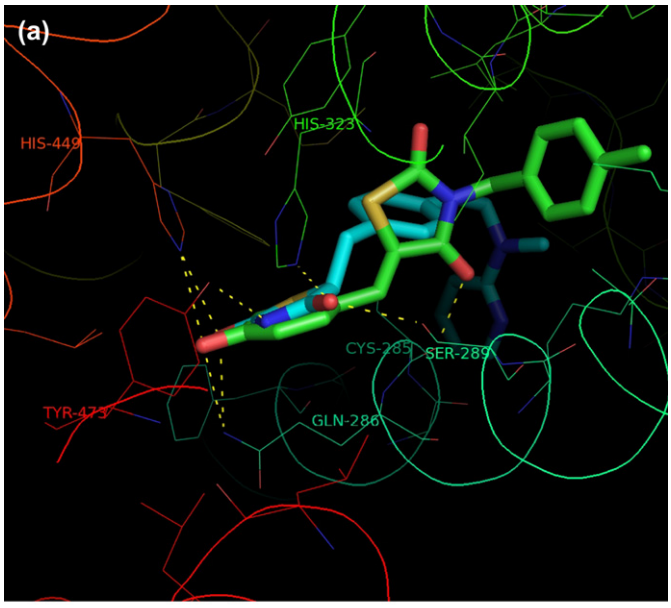

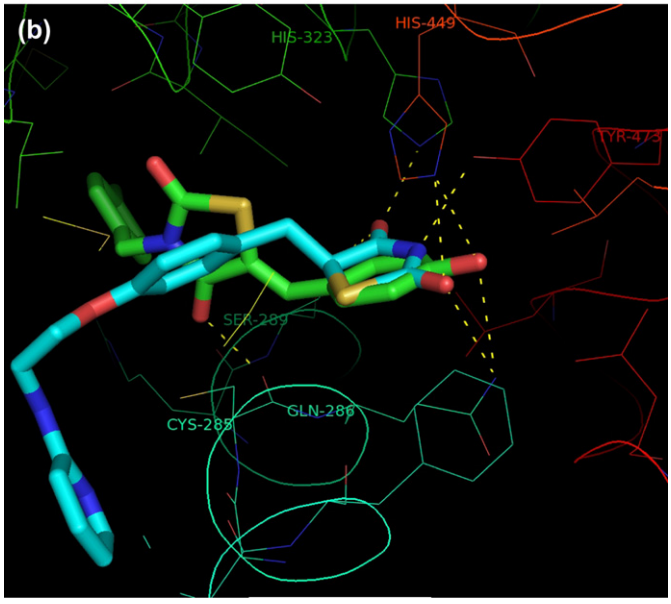

Fig. 4. Front (a) and back (b) view of important polar interactions between (*Z*) 5-(4-hydroxy-benzylidene)-3-(4-methyl-benzyl)-thiazolidine-2,4-dione **2** (green stick model) and the co-crystallized rosiglitazone (blue stick model), and PPAR-γ (wireframe model). The important residues involved are labelled.

of this figure reveals that for ligands **1** and **6**, the arylidene moiety was found oriented to the left side of the active site, while for ligand **3**, it is turned to the right side. Additionally, the structures are quite superposed. The slight differences observed between the free energies of binding for these 3 ligands, mainly for ligands **3** and **6** (same free energy of binding in PPAR-γ), cause a challenging interpretation of their biological differences in terms of the individual molecular structures, and further theoretical and experimental studies are needed, particularly the determination of ED_{40} for other molecules of this series, in order to permit a massive interpretation of the molecular aspects that induce these broad hypoglycemic and hypolipidemic activities.

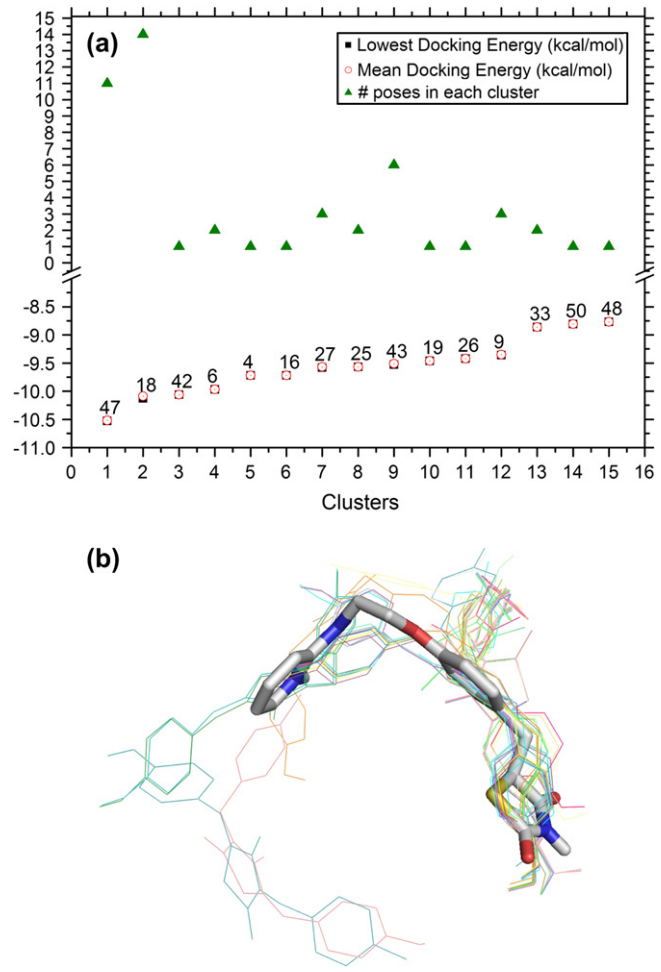

Fig. 5. (a) Cluster distribution of the docking solutions for ligand **2** in PPAR-γ. The results are organized into 15 clusters (RMS within 0.5 Å), each one with the lowest and mean docking energy and the number of poses. The numbers above the points represent the pose identification for the best result in each cluster; (b) superposition of the 50 docking poses (wireframe models), besides the crystallographic structure of the rosiglitazone (stick model).

7. Experimental protocols

7.1. (Z) 5-Benzylidene-3-(4-methyl-benzyl)-thiazolidine-2,4-diones: general procedure

A mixture of 3-(4-methyl-benzyl)-thiazolidine-2,4-dione (0.59 g, 2.5 mmol) and ethyl-(2-cyano-3-phenyl)-acrylate (2.7 mmol) is refluxed for 2–6 h in absolute ethanol (20 mL) with added piperidine (0.25 mL). After cooling, precipitates are purified by column chromatography or crystallized in suitable solvents. C, H, N, O analyses were within ±0.4% of the theoretical values.

7.2. (Z) 5-(4-Hydroxy-benzylidene)-3-(4-methyl-benzyl)-thiazolidine-2,4-dione ***2***

$C_{18}H_{15}NO_3S$, yield: 38%. Mp: 194–196 °C. TLC (chloroform) R_f: 0.68. IR (KBr; ν cm^{-1}) 3325, 1720, 1655, 1575, 1510, 1365, 1330, 1130, 825. ^1H NMR (δ ppm, DMSO-d_6): 2.25

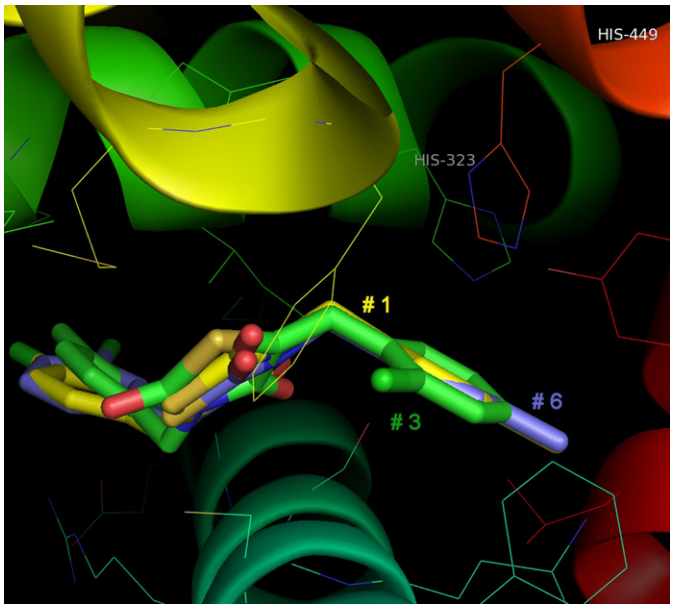

Fig. 6. Docking poses for ligands **1**, **3** and **6** in PPAR-γ. Important residues are labelled to facilitate the localization of these poses on the active site region.

(s, CH_3), 4.76 (s, NCH_2), 7.85 (s, CH), 7.16 (m, 4H benzyl), 6.92 (d, 2H benzylidene, $J = 8.1$ Hz), 7.48 (d, 2H benzylidene, $J = 8.4$ Hz), 10.4 (sl, OH). MS, *m/z* (%): 325 ($M^{+\bullet}$ 100), 326 (29.1), 312 (6.3), 105 (61.7).

7.3. (Z) 5-(3-Chloro-benzylidene)-3-(4-methyl-benzyl)-thiazolidine-2,4-dione ***6***

$C_{18}H_{14}ClNO_2S$, yield: 50%. Mp: 143–145 °C. TLC (*n*-hexane/ethyl acetate; 70:30) R_f: 0.8. IR (KBr; ν cm^{-1}) 3040, 2935, 1730, 1675, 1605, 1420, 1370, 1320, 1135, 920. ^{1}H NMR (δ ppm, DMSO-d_6): 2.27 (s, CH_3), 4.79 (s, CH_2), 7.16 (d, 2H, benzyl, $J = 8.4$ Hz), 7.21 (d, 2H, benzyl, $J = 8.4$ Hz), 7.58 (m, 3H, benzylidene), 7.73 (s, 1H, benzylidene), 7.96 (s, CH). MS, *m/z* (%): 343 ($M^{+\bullet}$ 55.4), 344 (11.6), 345 (16.6), 105 (100).

7.4. (Z) 3-(4-Methyl-benzyl)-5-(4-methyl-benzylidene)-thiazolidine-2,4-dione ***7***

$C_{19}H_{17}NO_2S$, yield: 45%. Mp: 139–140 °C. TLC (*n*-hexane/ethyl acetate; 70:30) R_f: 0.78. IR (KBr; ν cm^{-1}) 3010, 2930, 1730, 1675, 1590, 1425, 1370, 1320, 1135, 805.

Table 3
Effective doses for a 40% reduction (ED_{40}) of GP and TG in case of ATZDs **1**–**4** and **9** in mice with alloxan-induced diabetes and free energy of binding (ΔG) to PPAR-γ and PPAR-α

ATZD #	MW	ED_{40} PG, 10^{-5} mol/L	ΔG (kcal/mol), PPAR-γ	ED_{40} TG, 10^{-5} mol/L	ΔG (kcal/mol), PPAR-α
1	343	6.9	−8.36	5.8	−8.56
2	325	4.2	−8.90	–	−8.13
3	343	3.3	−8.61	8.8	−7.95
4	339	5.6	−8.36	0.97	−7.63
9	352	4.3	−8.85	5.8	−8.69

^{1}H NMR (δ ppm, DMSO-d_6): 2.27 (s, CH_3), 2.36 (s, CH_3), 4.79 (s, CH_2), 7.15 (d, 2H, benzyl, $J = 8.1$ Hz), 7.2 (d, 2H, benzyl, $J = 8.4$ Hz), 7.36 (d, 2H, benzylidene, $J = 8.1$ Hz), 7.53 (d, 2H, benzylidene, $J = 8.1$ Hz), 7.93 (s, CH). MS, *m/z* (%): 323 ($M^{+\bullet}$ 100), 324 (18.7), 325 (7.3), 105 (45.3), 91 (6.3).

7.5. (Z) 5-(3-Bromo-benzylidene)-3-(4-methyl-benzyl)-thiazolidine-2,4-dione ***8***

$C_{18}H_{14}BrNO_2S$, yield: 48%. Mp: 109–111 °C. TLC (benzene/ethyl acetate; 95:5) R_f: 0.9. IR (KBr; ν cm^{-1}) 2911, 1743, 1692, 1600, 1427, 1376, 1325, 758. ^{1}H NMR (δ ppm, DMSO-d_6): 2.28 (s, CH_3), 4.79 (s, CH_2), 7.16 (d, 2H, benzyl, $J = 8.1$ Hz), 7.22 (d, 2H, benzyl, $J = 8.1$ Hz), 7.4–7.45 (m, 1H, benzylidene), 7.54–7.6 (m, 2H, benzylidene), 7.82 (d, 1H, benzylidene, $J = 8.4$ Hz), 8.02 (s, CH). MS, *m/z* (%): 387 ($M^{+\bullet}$ 34.6), 389 (21.6), 308 (25.7), 212 (6.1), 132 (19.8), 105 (100), 89 (80.4), 77 (14.4).

7.6. (Z) 3-(4-methyl-benzyl)-5-(4-nitro-benzylidene)-thiazolidine-2,4-dione ***12***

$C_{18}H_{14}N_2O_4S$, yield: 39%. Mp: 189–191 °C. TLC (*n*-hexane/ethyl acetate; 70:30) R_f: 0.56. IR (KBr; ν cm^{-1}) 2360, 1743, 1692, 1614, 1509, 1380, 1148, 840. ^{1}H NMR (δ ppm, DMSO-d_6): 2.28 (s, CH_3), 4.81 (s, CH_2), 7.16 (d, 2H, benzyl, $J = 8.1$ Hz), 7.22 (d, 2H, benzyl, $J = 7.8$ Hz), 7.9 (d, 2H, benzylidene, $J = 9$ Hz), 8.35 (d, 2H, benzylidene, $J = 9$ Hz), 8.08 (s, CH). MS, *m/z* (%): 354 ($M^{+\bullet}$ 100), 355 (13.5), 326 (5.6), 105 (35.7), 89 (6.6).

Acknowledgments

We thank the CNPq (Conselho Nacional de Desenvolvimento Científico e Tecnológico, Brasil) and the CAPES/COFECUB (Fundação Coordenação de Aperfeiçoamento de Pessoal de Ensino Superior/Comité Français d'Évaluation de la Coopération Universitaire avec le Brésil) for their support.

References

[1] S. Ebdrup, I. Pettersson, H.B. Rasmussen, H.-J. Deussen, A.F. Jensen, S.B. Mortensen, J. Fleckner, L. Pridal, L. Nygaard, P. Sauerberg, J. Med. Chem. 46 (2003) 1306–1317.
[2] P. Sauerberg, I. Pettersson, L. Jeppesen, P.S. Bury, J.P. Mogensen, K. Wassermann, C.L. Brand, J. Sturis, H.F. Woldike, J. Fleckner, A.S. Andersen, S.B. Mortensen, L.A. Svensson, H.B. Rasmussen, S.V. Lehmann, Z. Polivka, K. Sindelar, V. Panajotova, L. Ynddal, E.M. Wulff, J. Med. Chem. 45 (2002) 789–804.
[3] J. Cobb, I. Dukes, Annu. Rep. Med. Chem. 33 (1998) 213–221.
[4] S.A. Grover, L. Coupal, H. Zowall, M. Dorais, Circulation 102 (2000) 722–727.
[5] C.J. Balley, Trends Pharmacol. Sci. 21 (2000) 259–265.
[6] C. Day, Diabet. Med. 16 (1999) 179–792.
[7] B.M. Spiegelman, Diabetes 47 (1998) 507–514.
[8] Y. Iwata, S. Miyamoto, M. Takamura, H. Yanagisawa, A. Kasuya, J. Mol. Graph. Model. 19 (2001) 536–542.
[9] P.J. Boyle, A.B. King, L. Olansky, A. Marchetti, H. Lau, R. Magar, J. Martin, Clin. Ther. 24 (2002) 378–396.

[10] J. Chilcott, P. Tappenden, M.L. Jones, J.P. Wight, Clin. Ther. 23 (2001) 1792–1823.
[11] R.T. Nolte, G.B. Wisely, S. Westin, J.E. Cobb, M.H. Lambert, R. Kurokawa, M.G. Rosenfeld, T.M. Willson, C. Glass, Nature 395 (1998) 137–143.
[12] J. Uppenberg, C. Svensson, M. Jaki, G. Bertilsson, L. Jendeberg, A. Berkenstam, J. Biol. Chem. 273 (1998) 31108–31112.
[13] J.L. Oberfield, J.L. Collins, C.P. Holmes, D.M. Goreham, J.P. Cooper, J.E. Cobb, J.M. Lenhard, E.A. Hull-Ryde, C.P. Mohr, S.G. Blanchard, D.J. Parks, L.B. Moore, J.M. Lehmann, K. Plunket, A.B. Miller, M.V. Milburn, S.A. Kliewer, T.M. Willson, Proc. Natl. Acad. Sci. U.S.A. 96 (1999) 6102–6106.
[14] T.M. Willson, J.E. Cobb, D.J. Cowan, R.W. Wiethe, I.D. Correa, S.R. Prakash, K.D. Beck, L.B. Moore, S.A. Kliewer, J.M. Lehmann, J. Med. Chem. 39 (1996) 665–668.
[15] I.R. Pitta, S.L. Galdino, M.C.A. Lima, J. Barbe, Brazilian Pat. PI-0300997-1, Rev. Propr. Intelect., no. 1695, 2003.
[16] V.L.M. Guarda, M.A. Pereira, C.A. De Simone, J.C. Albuquerque, S.L. Galdino, J. Chantegrel, M. Perrissin, C. Beney, F. Thomasson, I.R. Pitta, C. Luu-Duc, Sulfur Lett. 26 (2003) 17–27.
[17] S.F. Tan, K.P. Ang, Y.F. Fong, J. Chem. Soc. Perkin Trans. II (1986) 1941–1944.
[18] J.F.C. Albuquerque, A. Albuquerque, C.C. Azevedo, F. Thomasson, S.L. Galdino, J. Chantegrel, M.T.J. Catanho, I.R. Pitta, C. Luu-Duc, Pharmazie 50 (1995) 387–389.
[19] R.H. Mourão, T.G. Silva, A.L.M. Soares, E.S. Vieira, J.N. Santos, M.C.A. Lima, V.L.M. Lima, S.L. Galdino, J. Barbe, I.R. Pitta, Synthesis and biological activity of novel acridinylidene and benzylidene thiazolidinediones, Eur. J. Med. Chem. 40 (2005) 1129–1133.
[20] M.J.S. Dewar, E.G. Zoebisch, E.F. Healy, J.J.P. Stewart, J. Am. Chem. Soc. 107 (1985) 3902–3909.
[21] G.M. Morris, D.S. Goodsell, R.S. Halliday, R. Huey, W.E. Hart, R.K. Belew, A.J. Olson, J. Comput. Chem. 19 (1998) 1639–1662.
[22] M.F. Sanner, J. Mol. Graph. Model. 17 (1999) 57–61.
[23] H.E. Xu, M.H. Lambert, V.G. Montana, K.D. Plunket, L.B. Moore, J.L. Collins, J.A. Oplinger, S.A. Kliewer, R.T. Gampe Jr., D.D. Mckee, J.T. Moore, T.M. Willson, Proc. Natl. Acad. Sci. U.S.A. 98 (2001) 13919–13924.
[24] A.C. Wallace, R.A. Laskowski, J.M. Thornton, Protein Eng. 8 (1995) 127–134.
[25] DeLano W.L., The PyMOL Molecular Graphics System (2002) DeLano Scientific, San Carlos, CA, USA, <http://www.pymol.org>.
[26] S.F. Souza, P.A. Fernandes, M.J. Ramos, Proteins: Struct., Funct., Bioinf. 65 (2006) 15–26.